Available online www.jsaer.com

***Journal of Scientific and Engineering Research*, 2022, 9(11):131-140**

Research Article

ISSN: 2394-2630
CODEN(USA): JSERBR

Influence of CO_2 desorption on spirulina culture in a vacuum column

Djimako Bongo, Edith kadjangaba, Nekoulnang Djetounako Clarisse, Mbailaou Ngoussou, Salif Gaye, Jean-Yves Champagne

[1]Mechanical Engineering Department,Higher Normal School of Technology Sarh, Sarh, Chad
[2]Faculty of Sciences and Techniques, University of Doba, Doba, Chad
[3]Paleontology Department, National Research Center for Development of N'djamena, N'djamena, Chad.
University of sarh, Department of Chemistry, sarh, Chad
[4]LME Materials and Energetics Laboratory, University Institute of Technology, Thiès, Senegal
[5]Laboratory of Fluid Mechanics and Acoustics INSA-Lyon, Lyon, France
Email: djimako.b5@gmail.com

Abstract The evaluation of mass transfer function of vacuum column is performed experimentally by CO_2 stripping process. The experiment is conducted on previously described experimental setup Figure 1, incorporating necessary instruments for CO_2 injection and concentration measurement. A Metler Toledo CO_2 probe model Inpro5000 for on-line measurement of dissolved CO_2 concentration of liquid is used. The material exchange capacities between water and air within airlift are studied by following carbon dioxide concentrations in basin associated with column over time. This desorption or stripping operation consists in progressively extracting dissolved solute initially present in water by injecting air into bubble column. To do this, carbon dioxide is injected into raceway through a ceramic bubble diffuser immersed in raceway water supersaturated with CO_2. Starting from an initial concentration of solute in raceway, the column under vacuum is started. The evolution of CO_2 concentration in liquid phase is measured every two minutes during one hour of operation in loop of column. The measurement is made with a CO_2 probe (Metler Toledo) fixed on return line from column to raceway. CO_2 desorption is evaluated for several operating configurations by varying air flow rate, flanging liquid inlet pipe into column to evaluate effect of liquid flow rate on desorption. After evaluating CO_2 stripping, a determination of mass transfer coefficient in overall system was made. Considering a perfect mixture in whole system working in closed circuit, the value of K_{La} is deduced from an instantaneous balance on studied system:

Keywords stripping, diffuser, Bubble diameter, bubble velocity, biomass

1. Introduction

Analysis of mass transfer capabilities of bubble column is performed on experimental setup presented in Figure 1. To better understand and quantify CO_2 degassing capabilities of this column, several air flow rates are experimentally tested with aim of observing their influence on desorption and identifying optimal flow rate for CO_2 degassing. Tests are conducted in fresh water at room temperature with an initial CO_2 concentration of 2.6 $mg.l^{-1}$ (dissolved CO_2). CO_2 is injected into recirculation tank until saturation is reached using a ceramic diffuser. As soon as saturation is reached (210 ppm), the tests start by turning on column and recording concentration with a Mettler probe every minute. These tests were conducted for an air flow rate varying between 5 and 35 $l.min^{-1}$ for water at 20◦C. Results obtained are represented in figure 15, it seems obvious from

these tests that injected air flow rate plays a primordial role during first 15 or 20 minutes of tests during which decrease in concentration of CO_2 is very rapid and strongly depends on injected air flow rate between 5 l.mn-1 and 20 l.mn^{-1}. Thereafter, a weak evolution of extraction capacity is observed from 25 l.min^{-1}. Everything suggests that increase of air flow does not have any more influence on extraction capacity. After 20 minutes of desorption, concentration reaches an asymptotic level of 0.04 g.l^{-1} except for flow rate of 5 l.mn^{-1} whose performances indicate a more reduced extraction kinetics. Desorption of CO_2 by airlift is affected by counter airlift effect noticed previously in hydrodynamic study of airlift under vacuum.

2. Description of experimental device

Experimental device studied consists of airlift column, a vacuum pump, an air bubble injection system, a collection tank and instrumentation to characterize hydrodynamic behavior [Barkai thesis]. This installation is schematically shown in Figure 1. Column has a circular cross-section composed of two concentric tubes of diameter 150 mm (outer tube) and 80 mm (inner tube). Height of column is 3 meters. It is connected to a recirculation basin (in black PVC) by two PVC pipes of 50 mm diameter connected, one to internal tube and other to external tube of airlift (for return to basin). This allows column to operate in a closed circuit. System uses a vacuum pump to create a water level difference between basin and column, which allows for hydraulic recirculation [Bongo, barrut 2012b]. Figure 1 is picture of experimental setup used. For characterization of dispersed phase of flow, a two-phase instrumentation composed of an optical bi-probe and differential pressure sensors is used. For characterization of liquid phase, an ultrasonic flow meter is used.

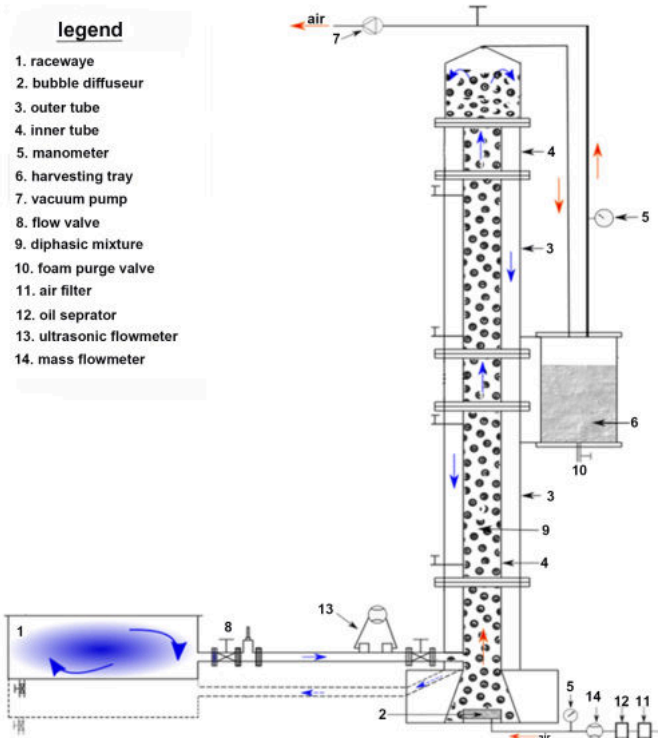

Figure 1: Experimental setup

2.1. Experimental Protocol

Bubble diameters will be measured for two different diffusers (ceramic and wood), in fresh and salt water.

1. Filling airlift with fresh water;

2. Positioning of diffuser (wood or ceramic) at bottom of aquarium, weighed down with a weight. This diffuser is connected to syringe by a flexible tube;
3. Position camera facing aquarium, above diffuser, and connect it to computer;
4. Lights on diffuser;
5. Start air flow with syringe pump at a speed of 0.8 mm. min-1 ;
6. Adjustment of focal distance of objective with respect to bubbles coming out of diffuser;
7. Camera settings (acquisition frequency and resolution);
8. Visualization of bubbles on screen, via Photron software of camera

2.2 Key factor of the column operation

Size of bubbles is a key factor in operation of air-lift vacuum column. Smaller and more numerous bubbles, larger gas-liquid exchange surface, and therefore better efficiency of system. Even if bubbles tend to coalesce after a certain height, bubble diffuser used is important, and it is necessary to differentiate between different existing diffusers in order to select most efficient ones for bubble column. There are several commercially available diffusers: A diffuser made of plastic, recreating a porous material, creating fine bubbles; A rubber diffuser, creating fine bubbles; A wooden diffuser, creating very fine bubbles (figure 2); A ceramic diffuser, creating micro-bubbles (figure 3). However, after having tested all these diffusers with naked eye, only ones diffusing very small bubbles are wooden and ceramic ones. This is why only these two diffusers will be studied at first, as they are most interesting ones for study of mass transfer.

Figure 2: Wooden diffuser

Figure 3: Ceramic diffuser

3. Results and Discusion

3.1. Average local diameter of CO_2 bubbles

Average bubble diameter, determined using optical bi-probe, is shown in (Figures 4; 5; 6 and 7) giving diameter in millimeters. Across all tests, bubble diameter increases with surface velocity of gaz and varies between 3 and 8 mm. It is characterized by a uniform population of small bubbles that rise vertically in column, without interacting with each other and with a low radial dispersion. In this regime, coalescence and rupture phenomena are negligible and diameter depends essentially on configuration of air diffusers and physicochemical properties of dispersion [Zahradnik et al., 1997]; [Simonnet, 2005]. The homogeneity of bubble size also shows that at a

height of 1 m, dispersed phase distribution is independent of radial location of air diffusers. These observations are consistent with widely accepted assumption for a mono-disperse bubble regime for low void rates [Lucas et al., 2005, Tomiyama, 1998].

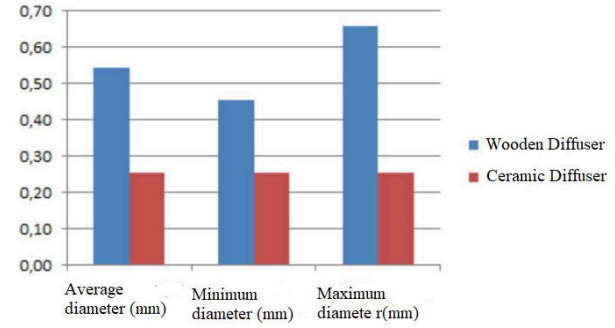

Figure 4: Bubble diameter in freshwater

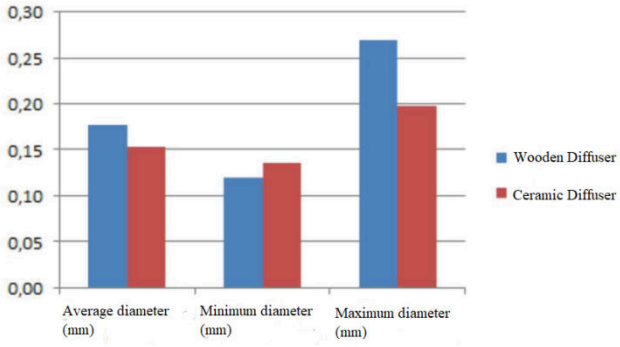

Figure 5: Bubble diameter in seawater

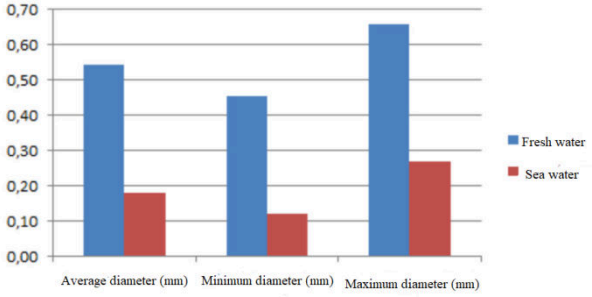

Figure 6: Bubble diameter for wooden diffuser

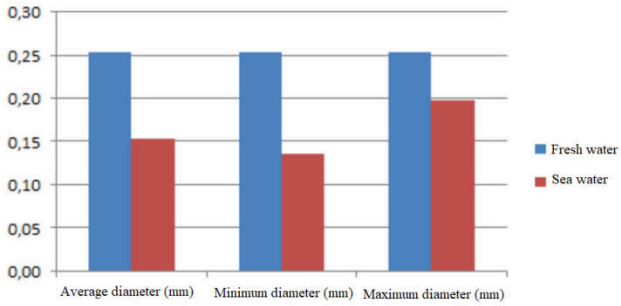

Figure 7: Bubble diameter for ceramic diffuser

3.2. Influence of salinity

Remembering the different behavior of airlift columns in seawater and freshwater, i.e. bubble size and gas retention, degassing rates in freshwater and seawater are close regardless of type of diffusers used. Barrut (2010a,) also showed that salinity has no influence on efficiency of material transfers. He suggested that this is due to low degassing efficiency of airlift. In seawater, the lack of bubble coalescence results in a smaller average bubble diameter than in fresh water (Fig. 7). Thus, interfacial area is large, interactions are more efficient and collected foam is more concentrated. Figure 8 shows influence of salinity on concentration efficiency of microalgae. There is an almost linear positive relationship between increasing salinity and concentration index. In seawater from 35 ‰, CI is about 8 times higher than in fresh water

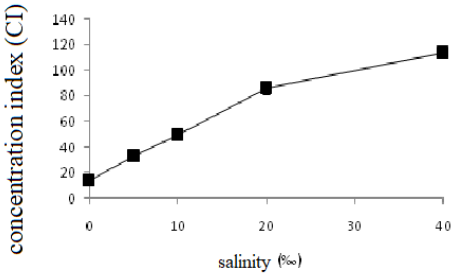

Figure 8: Influence of salinity on concentration efficiency

3.3. Local bubble rise velocity

The results of bubble ascent velocity measurements are presented as a function of gaz surface velocity. They show a homogeneous radial velocity profile except for height h = 1 m in presence of fresh water and h = 2 m in demineralized water. For low surface velocities, gaz is injected uniformly into column, flow regime is homogeneous and is characterized by a uniform population of small bubbles rising in column at same velocity (Figure 9; 10), without interacting with each other and with low radial dispersion for fresh water in accordance with observations of [Zahradník et al., 1997]. With demineralized water (Figures 10; 12), homogeneous regime corresponds to results obtained for velocity lower than 0, 36 m/s for which liquid velocity and gaz fraction increase linearly with injected gas flow rate. For these surface velocities, it is possible to state that velocity reapartition is closer. It is only for larger Ug values (Figure 9) that we start to observe a flow with higher velocities of dispersed phase that are localized in center of column. In this regime, clusters of bubbles or merged bubbles form central spiraling bubble flow, dragging with them a movement of continuous phase also spiraling in central area. The quality of water seems to have a significant effect on local speed of bubble ascent, which is greater in demineralized water than in fresh water (figures 10; 12; 4 and 7). This difference is more pronounced at 2 m height: Vg = 0.75 $m.s^{-1}$ in fresh water and V_l = 1.16 $m.s^{-1}$ in demineralized water, which gives a difference of 46%. These results are in agreement with literature where it is commonly accepted that rate of ascent decreases when water is contaminated [Clift et al., 1978], it is same for coalescence that also depends on impurities present in water. As an example, figure 13 represents terminal velocity of an isolated bubble in a liquid phase at rest for different two-phase flow regimes [Clift et al.] For bubbles of average diameter between 4 mm and 6 mm, terminal velocity varies between 0, 25 $m.s^{-1}$ and 0, 18 $m.s^{-1}$ respectively for pure water and contaminated water.

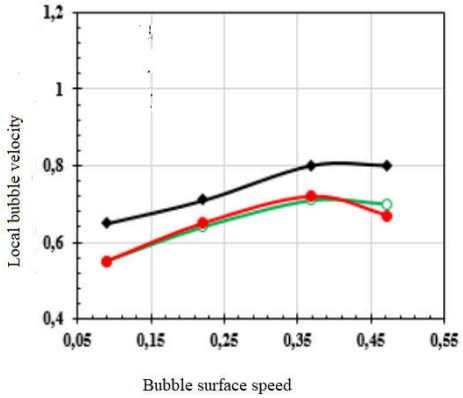

Figure 9: Influence of fresh water on velocity evolution (h=1m)

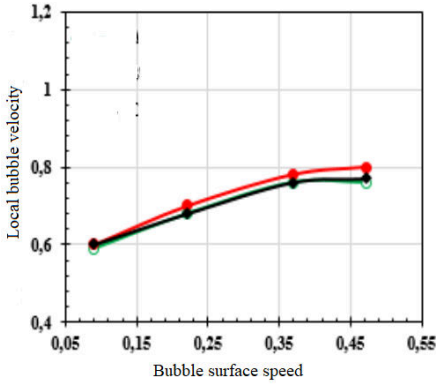

Figure 10: Influence of demineralized water on velocity evolution (h=2m)

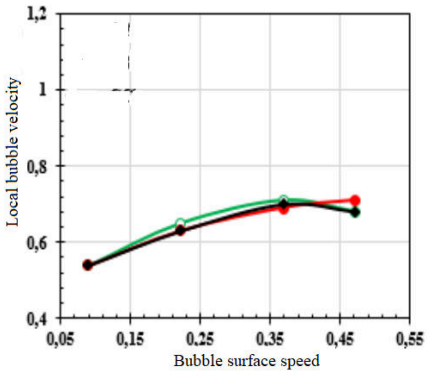

Figure 11: influence of fresh water and height on velocity evolution

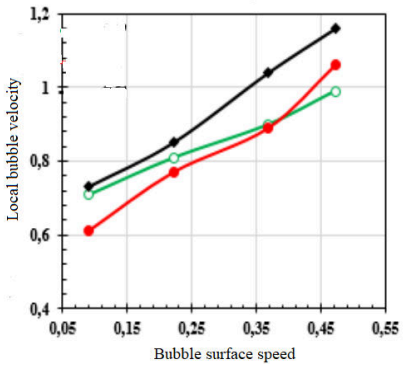

Figure 12: Influence of demineralized water and height on the evolution of velocities

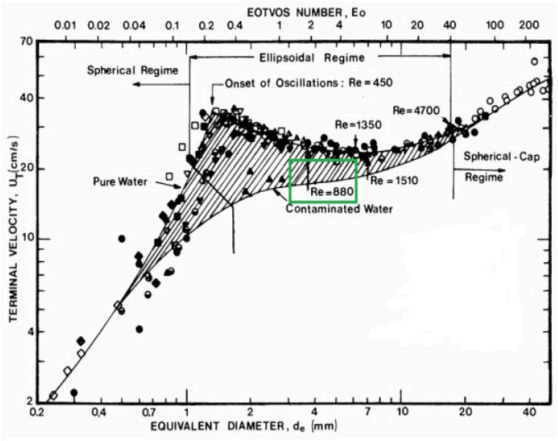

Figure 13: Terminal bubble velocity in water at 20°C (Clift et al., 1978)

3.4. Local void rate

Local void rate is deduced from one of two optrodes of optical bi-probe by distinguishing time it remains exposed to gas from time it is in liquid medium. Presented in Figure 14 for fresh water and demineralized water respectively. It can be seen that for section 1, local void rate is relatively homogeneous except for a high velocity, thus a high air flow, for which a slight dissymmetry begins to be observed which seems to be slightly

more marked for demineralized water. This distribution extends to section 2 with however a more marked dissymmetry for demineralized water at high air flow

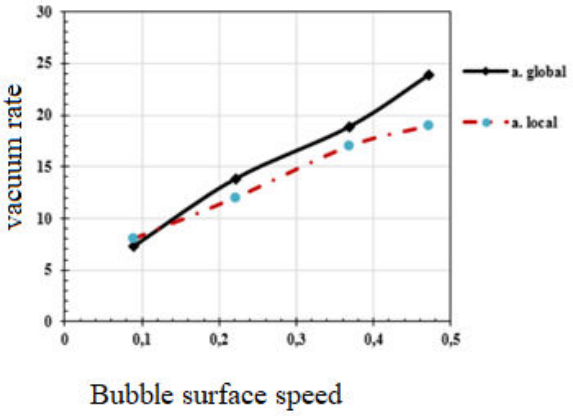

Figure 14: Evolution of void rate as a function of bubble velocity

4. Dissolution of CO_2

Material exchange capacity between water and air at airlift column is studied over time Figure 15. This desorption or stripping consists in progressively extracting dissolved solute present in water by injecting air into bubble column. To do this, carbon dioxide is injected into raceway through a ceramic bubble diffuser immersed in water supersaturated with CO_2. Starting from an initial solute concentration in raceway, vacuum column is started. The evolution of CO_2 concentration in liquid phase is measured periodically (2mn) during one hour of operation in closed loop of column. The measurement is made with a Metler Toledo CO_2 probe fixed on return line from airlift to raceway. CO_2 desorption is evaluated for several operating configurations by varying air flow rate, flanging liquid inlet pipe into column to evaluate effect of liquid flow rate on desorption. After evaluating CO_2 stripping, a determination of mass transfer coefficient K_{La} in overall system was made. Considering a perfect mixture in whole system operating in closed circuit, value of K_{La} is deduced from an instantaneous balance on studied system

$$dCL/dt = KLa * (C_S - C_L) \quad (1)$$

The results of analysis of CO_2 desorption capacity of vacuum airlift show that CO_2 stripping speed increases during first 15 minutes with air flow rate during operation of airlift. Mass transfer coefficients obtained indicate that desorption of CO_2 by airlift is also affected by counter airlift effect which appears for air flow rates higher than 30 $l.mn^{-1}$.

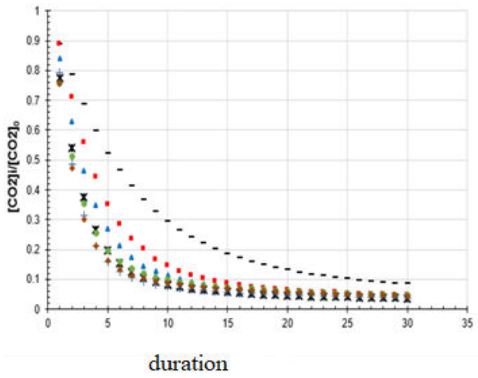

Figure 15: The influence of time on stripping

5. Conservation of the Mass

Mass of carbon dioxide injected into airlift is partially dissolved (Figure 16, a), in liquid phase and remaining part is directly released into atmosphere, as shown in equation (2). The continuously injected air shown in Figure (16, b) also results in a reduced mass of carbon dioxide dissolved in liquid in atmosphere. The carbon dioxide dissolved in liquid phase will either be transformed into biomass [3; 4; 5] or will remain in dissolved form in liquid, as described by mass balance written in equation (3).

$$m\_injected = mundiss + mdiss \quad (2)$$

$$m\_diss = mdepleted + mresidual + m(CO_2 \text{ converted to biomass}) \quad (3)$$

Dissolving CO_2 a Striping rogression b

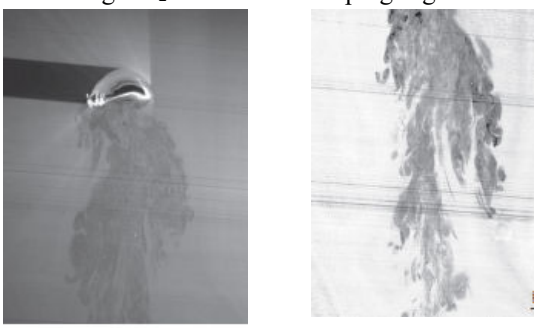

Figure 16: Diagram of carbon dioxide dissolution phase (a) and the continuous air stripping phase (b).

Dividing equation (3) by mass of carbon dioxide injected, we obtain equation (4) regarding mass transfer efficiency (MTE) of airlift Figure.17. The conversion of airlift CO_2 to biomass ETM, ηCO_2 converted to biomass, is defined as ratio of mass of carbon dioxide contained in dry mass of microalgae at outlet (mCO_2 converted to biomass) to mass of carbon dioxide injected (minjected). Similarly, dissolved yield (ηdiss), stripped yield (η stripped), and residual yield (η residual) are defined as ratios of m diss, m stripped, and m residual to injected mass (m injected), respectively.

$$\eta\ (CO_2 \text{ converted to biomass}) = \eta diss - \eta depleted - \eta residual \quad (4)$$

In following sections, dissolution and extraction phases are modeled as a function of process parameters.

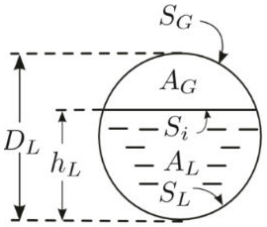

Figure 17: Notations according to Taitel .

Performance measurements are a function of injected gas concentration but also of flow regimes through mass transfer coefficients and gaz-liquid contact time. Therefore, mass transfer efficiencies (MTEs) must be measured for operational conditions of injected gas, i.e., concentration of flue gaz relevant to our application, as was done in [10], for an outdoor microalgae culture. Concerning mass transfer models, most often global mass transfer coefficients or volumetric mass transfer coefficients are correlated to process parameters [11; 12; 13; 14]. To our knowledge, there is no mass transfer model in literature relating mass of carbon dioxide injected to biomass produced in an airlift column.

6. Conclusion

Regarding results of analysis of CO_2 desorption capacity of airlift under vacuum, it is highlighted that CO_2 desorption rate increases with air flow rate during first 15 minutes of column operation. The mass transfer

coefficients obtained indicate that desorption of CO_2 by airlift is also affected by counter airlift effect which appears for air flow rates higher than 30 $l.mn^{-1}$. Analysis of bubble ascent speed obtained with an optical bi-probe shows that these speeds increase with vacuum rate.Water quality seems to have a significant effect on bubble ascent speed which is more important in demineralized water than in fresh water. It thus appears that evolution towards an increase or a decrease of coalescence, thus of bubble ascent rate, will depend on nature of impurities in water. There is also an underestimation of bubble ascent rate by optical bi-probe of about 50%. Results of various measurements indicate that water quality does not seem to have an effect on void rate as expected. Results of measurements at two measurement heights are very close and measurement position does not significantly influence void rate. However, in demineralized water, a slight asymmetry is observed, with a slightly higher void rate. Coalescence seems to have as much impact on bubble detection time as on bubble size, which would explain slight increase in void rate with altitude. Diameter of bubbles increases linearly with vacuum rate. It is larger in demineralized water than in fresh water, which confirms important influence of water quality observed earlier with bubble ascent rate.

References

[1]. Hassan, B, A.(2020). Caractérisation d'un écoulement diphasique dans un airlift sous dépression. Application pour l'extraction des matières solides en suspension. PhD thesis INSA- Lyon

[2]. Djimako B, Nekoulnag C, Jean-Mari M M, Alexis M N, Jean-Yves C, Salif G.(2019). Improvement of the Microalgae Harvest by the "Foaming-Scumming" Function of an Airlift Column. Open Journal of Fluid Dynamics, 9, 63-71.

[3]. Barrut, B., Blancheton, J.-P., Champagne, J.-Y., and Grasmick, A. (2012b). Water delivery capacity of a vacuum airlift–application to water recycling in aquaculture systems. Aquacultural engineering, 48 :31–39.

[4]. Zahradnik, J., Fialova, M., Ruzicka, M., Drahos, J., Kastanek, F., and Thomas, N. H. (1997). Duality of the gas-liquid flow regimes in bubble column reactors. Chemical Engineering Science, 52(21) :3811–3826.

[5]. Simonnet, M. (2005). Étude expérimentale du mouvement de bulles en essaim : application à la simulation numérique de colonnes à bulles. PhD thesis, Vandoeuvre-lesNancy, INPL.

[6]. Lucas, D., Krepper, E., and Prasser, H.-M. (2005). Development of co-current air–water flow in a vertical pipe. International Journal of Multiphase Flow, 31(12) :1304 – 1328

[7]. Tomiyama, A. (1998). Struggle with computational bubble dynamics. In •, editor, •. ICMF'98, Third International Conference on Multiphase Flow.

[8]. Barrut, B., Blancheton, J.-P., Champagne, J.-Y., and Grasmick, A. (2012a). Mass transfer efficiency of a vacuum airlift—Application to water recycling in aquaculture systems. Aquacultural Engineering, 46 :18–26

[9]. Zahradník, J., Fialová, M., Ružička, M., Drahoš, J., Kaš tánek, F., and Thomas, N. (1997). Duality of the gas-liquid flow regimes in bubble column reactors.Chemical Engineering Science, 52(21) :3811 – 3826

[10]. Clift, R., Grace, J. R., and Weber, M. E. (1978). Particles. Courier Corporation, New York, academic edition

[11]. L. Cheng, L. Zhang, H. Chen, C. Gao, Carbon dioxide removal from air by microalgae cultured in a membrane-photobioreactor, Separation and Purification Technology 50 (3) (2006) 324–329.

[12]. D. Ayhan, Biodiesel from oilgae, biofixation of carbon dioxide by microalgae : A solution to pollution problems, Applied Energy 88 (10) (2011) 3541–3547.

[13]. K. G. Zeiler, D. A. Heacox, S. T. Toon, K. L. Kadam, L. M. Brown, The use of microalgae for assimilation and utilization of carbon dioxide from fossil fuel-fired power plant flue gas, Energy Conversion and Management 36 (6-9) 707–712

[14]. J. Doucha, F. Straka, K. L´ıvansky, Utilization of flue gas for cultivation of microalgae ´ chlorella sp.) in an outdoor open thin-layer photobioreactor, Journal of Applied Phycology 17 (5) (2005) 403–12.

[15]. D. Baquerisse, Modelling of a continuous pilot photobioreactor for microalgae production, Journal of Biotechnology 70 (1-3) (1999) 335–342.

[16]. K. Loubiere, J. Pruvost, F. Aloui, J. Legrand, Investigations in an external-loop airlift photobioreactor with annular light chambers and swirling flow, Chemical Engineering Research and Design 89 (2) (2011) 164–171

[17]. R. Reyna-Velarde, E. Cristiani-Urbina, D. J. Hernandez-Melchor, F. Thalasso, R. O. ´ Ca˜ *n*izares-Villanueva, Hydrodynamic and mass transfer characterization of a flat-panel airlift photobioreactor with high light path, Chemical Engineering and Processing : Process Intensification 49 (1) (2010) 97–103.

[18]. L. Fan, Y. Zhang, L. Zhang, H. Chen, Evaluation of a membrane-sparged helical tubular photobioreactor for carbon dioxide biofixation by chlorella vulgaris, Journal of Membrane Science 325 (1) (2008) 336–345